Pharmaceutical Research, Vol. 24, No. 6, June 2007 (© 2007)
DOI: 10.1007/s11095-006-9229-5

Research Paper

Intracellular Kinetics of Non-Viral Gene Delivery Using Polyethylenimine Carriers

Jiaye Zhou,[1] James W. Yockman,[2] Sung Wan Kim,[1,2] and Steven E. Kern[1,2,3,4]

Received October 11, 2006; accepted December 22, 2006; published online March 27, 2007

Purpose. Polymeric nucleic acid carriers are designed to overcome one or more barriers to delivery. High molecular weight polyethylenimine (PEI) shows high transfection efficiency but exhibits high cytotoxicity (Fischer et al. *Biomaterials*, 24:1121–1131 (2003); Peterson et al. *Bioconjug. Chem.*, 13:845–854 (2002)). Nontoxic water-soluble lipopolymer (WSLP) was previously developed using branched poly(ethylenimine) (PEI, mw 1,800) and cholesteryl chloroformate (Han, Mahato, and Kim. *Bioconjug. Chem.*, 12:337–345 (2001)) and is an effective non-viral gene carrier with transfection levels equal or above high molecular weight PEI with a lower cytotoxicity profile. To understand how differences in these polymeric carriers influence transfection, we studied the pharmacokinetics of polymer gene carriers at the cellular level.

Materials and Methods. Cells were exposed in vitro to different polymeric carriers and the transport of the carriers into different cellular compartments was determined using cellular fractionation and real-time quantitative PCR. A multi-compartment mathematical model was applied to time series measurements of the trafficking of plasmids across each cellular barrier.

Results. Our result indicates that the chemical modification of WSLP increased the rate parameter for endosomal escape significantly compared to conventional PEI carriers thereby increasing the overall transfection efficiency.

Conclusions. These results are consistent with the goal of endosomal destabilization of the carrier design. This method provides a quantitative means for assessing different polymer construct designs for gene delivery.

KEY WORDS: cellular trafficking; computational model; gene delivery; kinetic analysis.

INTRODUCTION

Engineered non-viral polymeric nucleic acid delivery is an emerging pharmaceutical and therapeutic tool. Unlike traditional, small molecular weight agents that often exert their effect directly through exposure to the site of drug effect, nucleic acid delivery involves a series of biological processes at the cellular level that typically requires targeting a specific cellular location, such as the nucleus, for drug effect. Successful cellular targeting requires the delivery complex to overcome several major barriers including cell membrane binding, endocytosis, endosomal escape, and nuclear entry. Unfortunately synthetic polymeric gene delivery vectors are relatively inefficient in transfection comparing to viral counterparts. Thus, a clear understanding of how synthetic carriers behave at each of these barriers is crucial to future design optimization.

In vivo polymeric gene delivery often relies on local injection, resulting in localized pharmacokinetics. Therefore pharmacokinetic models defining dose/concentration relationships at a tissue and cellular level is necessary. Several quantitative studies at the cellular level have been reviewed (4–7). Banks *et al*. have provided a framework to analyze this multi-step uptake process involving external culture medium, cell cytoplasm, and the nucleus as compartments. For polymeric carriers that rely on either clathrin or receptor mediated endocytosis, cellular uptake is not a single step process. These delivery systems need to consider the kinetics of cell binding, endosomal uptake and endosomal release (Fig. 1). The kinetics at these steps are influenced by the chemical structure of the polymer carrier. Recently, Varga et al. reviewed quantitative comparison of several polyethylenimine (PEI) formulations to adenoviral vectors in cellular transport (6). Rate parameters at these steps were extrapolated for several PEI formulations based on total cell fractionation and nuclear extraction. This study showed that for small molecular weight PEI, endosomal escape appears to be rate limiting while the same is not true for high molecular weight PEI (i.e., PEI25K). While PEI25K exhibits high transfection efficiency, it has also shown high cytotoxicity therefore limiting its therapeutic use (1,2).

[1] Department of Bioengineering, University of Utah, Salt Lake City, Utah 84112, USA.
[2] Department of Pharmaceutics & Pharmaceutical Chemistry, University of Utah, 421 Wakara Way #318, Salt Lake City, Utah 84108, USA.
[3] Department of Anesthesiology, University of Utah, Salt Lake City, Utah 84132, USA.
[4] To whom correspondence should be addressed. (e-mail: Steven.Kern@hsc.utah.edu)

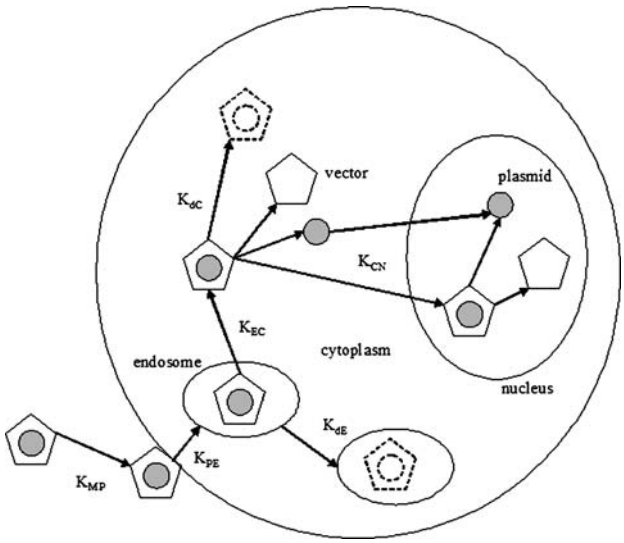

Fig. 1. Schematic diagram of the barriers described in the kinetic model. Polymer/plasmid complex binds to the plasma membrane (K_{MP}) and is internalized by endosomes (K_{PE}). Complex in the endosomes either escapes (K_{EC}) or undergoes degradation ($K_{>dE}$). Once inside the cytoplasm, the complex can dissociate and plasmid DNA enters the nucleus or the entire complex can enter the nucleus via diffusion or energy dependent mechanisms. This process is represented by a global kinetic marker (K_{CN}). Degradation in the cytoplasm also occurs (K_{dC}). Free plasmids inside the nucleus are then expressed.

We have previously designed a novel water soluble lipopolymer (WSLP, $mw = 20$ K) using PEI1.8K with direct conjugation of cholesteryl chloroformate (3). This carrier has shown non-toxicity and significant improvement in transfection efficiency over PEI1.8K. In this study, we explore the relationship of these chemical modifications to carrier pharmacokinetics of overcoming cellular barriers, especially endosomal escape comparing WSLP with PEI1.8K and PEI25K. Trans-gene content associated with the plasma membrane, endosome, and cytoplasm of transfected cells were collected via subcellular fractionation offering a higher resolution analysis building on previous studies. In addition, a mathematical analysis was conducted to determine the rate parameter change due to chemical modification of our polymers.

Our *in vitro* kinetic analysis establishes a basis for transfection kinetics in a homogeneous, well-mixed environment that represents an optimal *in vivo* scenario, and theoretical limit for *in vivo* transfection efficiency. To assess the impact of polymer carrier on gene delivery, transfected cells were collected and pDNA with each of the three carriers were isolated and quantified from each cellular compartment of interest. This approach can serve as a platform for analyzing appropriate formulations constructed for targeted gene-delivery systems to optimize their delivery to subcellular compartments.

MATERIALS AND METHODS

In vitro studies to assess the kinetics of non-viral gene delivery to different cellular compartments was undertaken by first synthesizing the WSLP polymer carrier and the plasmid of interest (pCMVIL-12). After *in vitro* incubation, cell culture plates were analyzed at serial time points to assess gene construct transport to different cellular regions.

Synthesis of WSLP

Synthesis of WSLP was described previously by Han *et al.* (3). Our procedure was slightly modified. Briefly, 3 g of PEI (Mw 1,800) was stirred on ice for 30 min in a 30 ml anhydrous chloroform and 100 μl anhydrous triethylamine (TEA). Cholesteryl chloroformate (1 g) was dissolved in 10 ml of ice cold anhydrous chloroform, and was added slowly to the PEI. The solvent was evaporated by stirring overnight, resulting in a viscous yellow gel. The gel was subsequently dissolved in a 50 ml 0.1N HCl and filtered through a glass membrane filter followed by a wash with 200 ml anhydrous chloroform to remove excess polymer and cholesterol. The WSLP containing aqueous layer was washed again with HCl and anhydrous chloroform as described above. The aqueous phase was lyophilized and the WSLP was recovered as a yellow powder.

pCMVIL-12 Plasmid Preparation

Plasmid pCMVIL-12 was constructed to contain subunit encoding gene mIL-12p35 driven by CMV promoter as previously described by Mahato *et al.* (8). Briefly, the p35 and p40 cDNAs are amplified by PCR using pIREmI-12 as a template. The amplified p35 and p40 cDNAs were inserted into pCI plasmid carrying a CMV promoter, resulting in the construction of pCMV-p35 and pCMV-p40. We isolate the p40 expression unit in pCMV-p40 and insert it into pCMV-p35 at a BamHI site. The pCMVmIL-12 construct is confirmed by a restriction enzyme essay.

Polymer and Plasmid Complexes

Polymers were mixed directly with pCMVIL-12 in the presence of 5% (w/v) glucose and water. Complex formation proceeded at room temperature for 30 min prior to transfection. PEI25000/pCMVIL-12 complex was prepared at N/P ratio of 5:1 (9). PEI1800/pCMVIL-12 and WSLP/pCMVIL-12 complexes (3) were prepared at N/P ratio of 15:1 (8).

In Vitro Transfection

For *in vitro* analysis, 10×10^6 B16-F0 (mouse melanoma) cells were transfected with 10 μg pCMVIL-12 using PEI25K, PEI1.8K, and WSLP. Cell samples were collected over time for up to 20 h after transfection. Levels of pDNA associated with each of the compartments were measured by subcellular fractionation, plasmid purification and subsequent real-time PCR. The B16-F0 cells were plated in T75 flasks in DMEM containing 10% FBS and antibiotics. The plates were incubated at 37°C and humidified 5% CO_2 until cells reached confluency (~80%). Cells were washed with serum-free DMEM medium and 10 ml fresh serum-free medium was added. PEI25000/pDNA, PEI1800/pDNA and WSLP/pDNA complexes were added to the cells. The final pDNA concentration in the media was 1 μg/ml. The cells were incubated for 4 h at 37°C and 5% CO_2. After 4 h, the transfection mixtures were replaced by 10 ml of fresh DMEM

containing 10% FBS. Cells were incubated for up to an additional 16 h. Cell samples were collected by trypsinzation at 1, 2, 4, 6, 10, 14, and 20 h time points.

Subcellular Fractionation

The transfected cells were re-suspended in 0.25 M sucrose, 10 mM Tris-HCl, 1 mM EDTA, pH 7.2. The suspension was homogenized using a ball-bearing homogenizer with 17 μ clearance. The homogenate was centrifuged for 10 min at 800×g. The supernatant was applied to 23% isotonic Percoll. The density gradient was centrifuged at 59,000×g for 25 min and fractionated with a peristaltic pump into 12 fractions (~1 ml). The pellet from the homogenization step was re-suspended in 0.25 M sucrose, 10 mM Tris-HCl, 1 mM $MgCl_2$, pH 7.5. The suspension was homogenized again with a Dounce homogenizer. Sucrose (2.4 M) with $MgCl_2$ was added to adjust the final sucrose concentration to 1.6 M. The above solution was overlaid with 0.25 M sucrose to setup a two layer sucrose gradient. The gradient was centrifuged at 70,900×g for 70 min. A band rich in nuclei was collected. Cell fractions were analyzed for hexosaminidase activity (lysosomal), 5′-nucleotidase activity (plasma membrane), lactate dehydrogenase activity (cytosolic) and ethidium bromide binding (nucleus) assays. The 12 fractions (excluding the nucleus) were pooled into three portions to capture over 85% of the protein activities representing plasma membrane, endosomes, and cytoplasm components.

TaqMan Realtime Quantitative PCR

Quantification of the plasmid DNA was performed with realtime PCR using the PE Biosystems Prism 7900 (Applied Biosystems, Foster City, CA, USA). Plasmid primers and probe were designed to contain the sequences: forward primer (5′-CGT GTC GCC CTT ATT CCC TTT-3′), reverse primer (5′-AAA CGC TGG TGA AAG TAA AAG ATG C-3′). PCR cycle conditions were 50°C for 2 min, 95°C for 10 min, and 40 cycles of 95°C for 15 s and 60°C for 1 min.

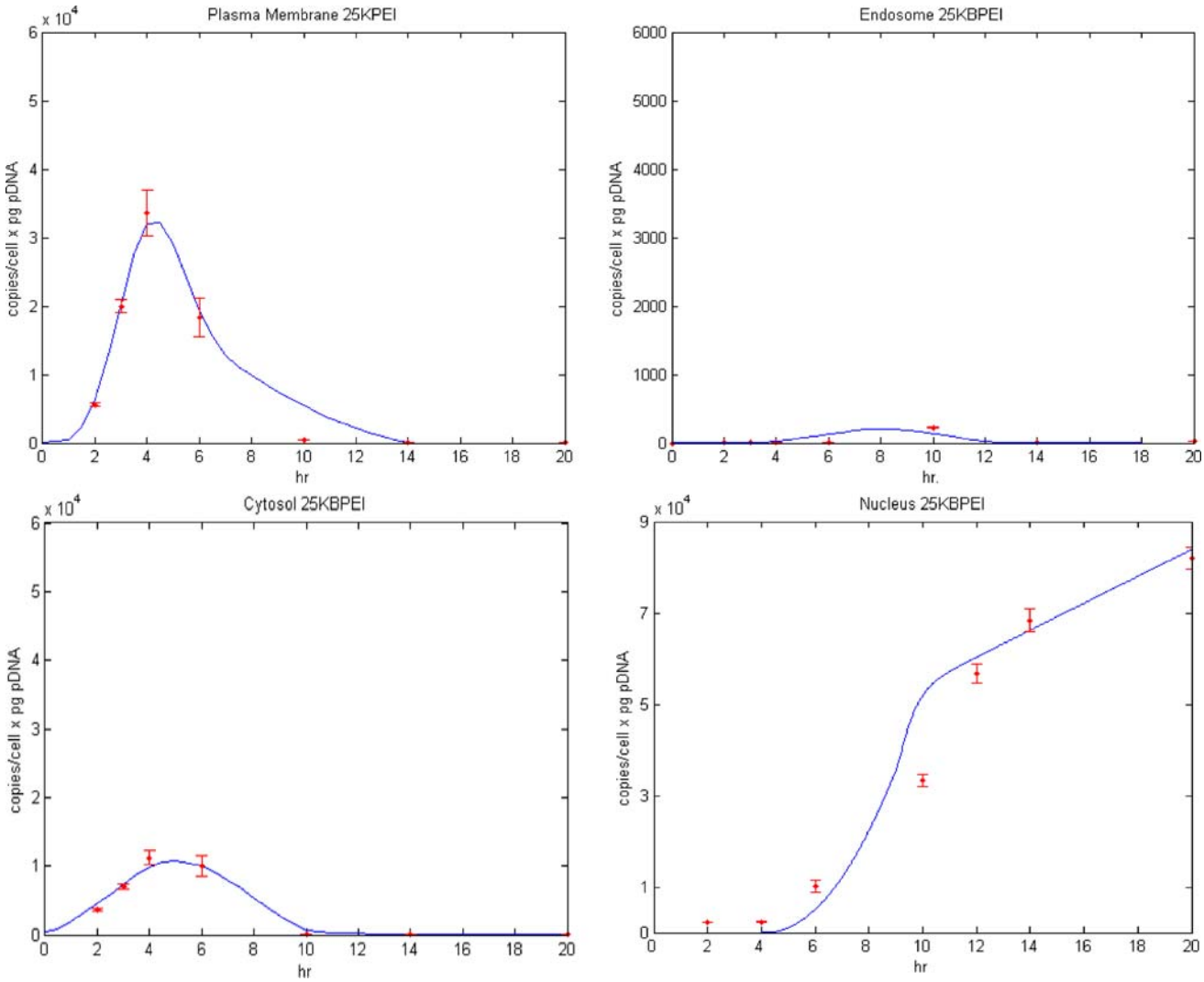

Fig. 2. Experimental result and parameter fitting curve of plasmid DNA equivalent time-lapse profile in each cellular compartment (plasma membrane, endosome, cytosol, and the nucleus). B16-F0 cells were transfected with 10 μg pCMVIL-12 complexed with PEI25K followed by subcellular fractionation and isolation of the plasmid DNA. Plasmid DNA equivalent are measured using realtime-PCR. Data are reported as mean ± SD of three experiments.

Negative control experiments that were not transfected are included to ensure specificity of the primers. Samples containing 10, 10^2, 10^3, 10^4, 10^5, 10^6 plasmid copies are include to construct the calibration curve.

Mathematical Modeling

The intracellular uptake and delivery of the plasmid DNA is a multi-step process across several cellular regions. A mathematical model was constructed as a number of consecutive first-order mass action events. First, the complex binds to the plasma membrane with rate constant k_{MP}. Next, the complex is taken up into the cell endosomal compartment at rate constant k_{PE}. The degradation of the plasmid DNA and endosomal escape are both modeled as first-order mass action events with rate contants k_{dE} and k_{EC} respectively. Transduction directly from the membrane into the cytosol, if any, is defined by k_{PC}. Degradation in the cytosol has the rate of k_{dC}. The uptake into the nucleus is modeled as a single first-order event with rate constant k_{CN}. This system is represented by the following series of first order differential equations:

$$\frac{dM}{dt} = -k_{MP}M$$

$$\frac{dP}{dt} = k_{MP}M - (k_{PE} + k_{PC} + k_{dP})P$$

$$\frac{dE}{dt} = k_{PE}P - (k_{EC} + k_{dE})E$$

$$\frac{dC}{dt} = k_{EC}E - (k_{CN} + k_{dC})C$$

$$\frac{dN}{dt} = k_{CN}C$$

The compartmental model was constructed using MatLab (MathWorks, Inc., Natick, MA, USA). Parameter estimation was performed using the MatLab Optimization Toolbox with a non-linear least-squares method to optimize rate constants, and System Biology Toolbox (http://www.sbtoolbox.org)

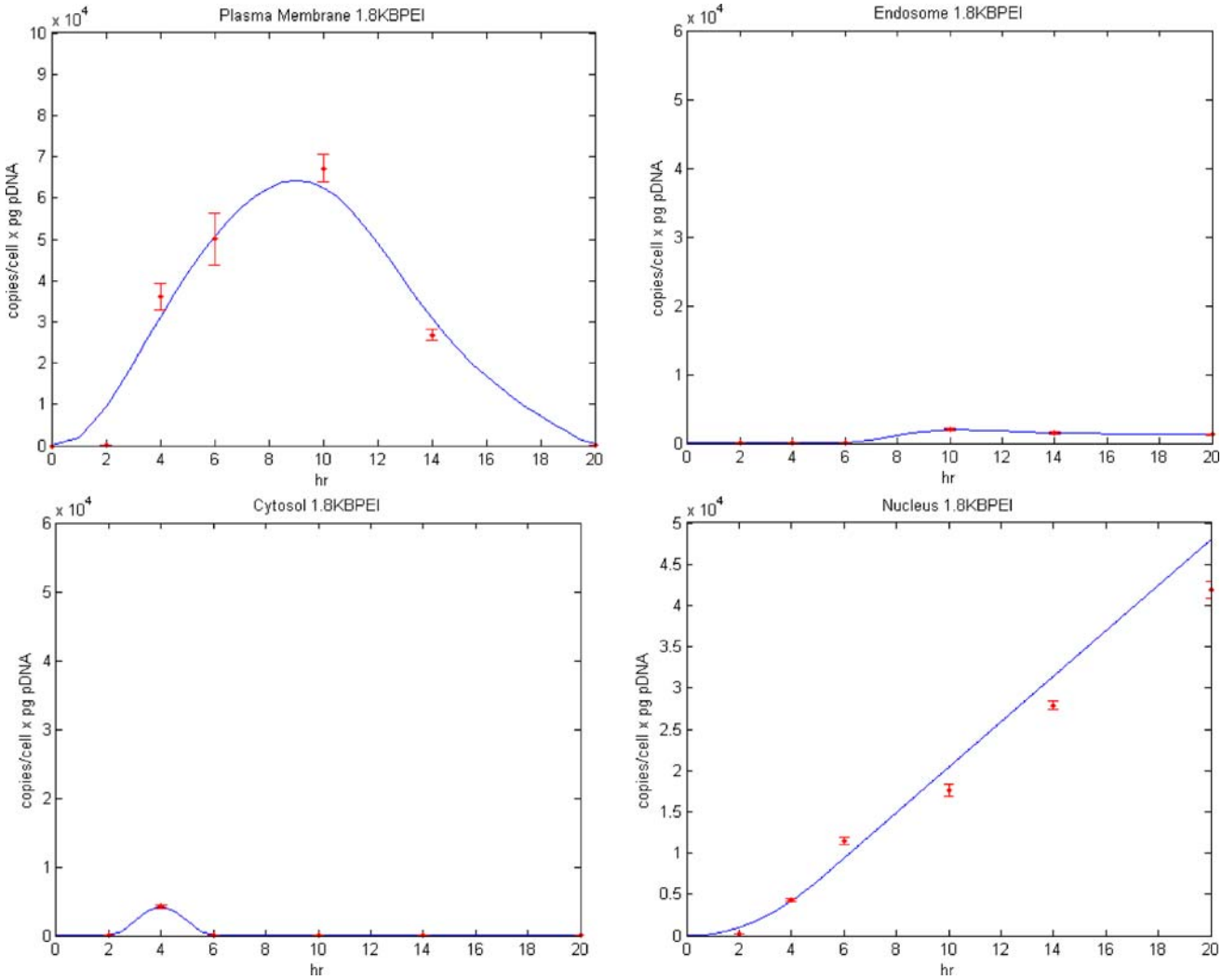

Fig. 3. Experimental result and parameter fitting curve of plasmid DNA equivalent time-lapse profile in each cellular compartment (plasma membrane, endosome, cytosol, and the nucleus). B16-F0 cells were transfected with 10 μg pCMVIL-12 complexed with PEI1.8K followed by subcellular fractionation and isolation of the plasmid DNA. Plasmid DNA equivalent are measured using realtime-PCR. Data are reported as mean ± SD of three experiments.

using Nelder-Mead downhill simplex optimization function using the plasmid concentration measurements made at serial time points of subcellular fractionation.

RESULTS

The fit of the measured experimental results to the model for parameter estimation is shown in Figs. 2, 3 and 4. Both the temporal and spatial profiles of the three polymers are similar. All three polymer carriers transfect cells following the same endosomal uptake and release pathway. In all three systems, there was significant accumulation of the pDNA associated with the plasma membrane. The pDNA then leaves the plasma membrane and enter the internal compartments of the cells. pDNA complexed with PEI25K enter into the cytoplasm quickly with some but insignificant transient accumulation inside the endosomal compartments. pDNA complexed with PEI1.8K showed prolonged accumulation inside the endosomes at a more moderate level, while significant less pDNA managed to enter the cytoplasm. pDNA complexed with WSLP shows accumulation in the endosomal compartments as well as in the cytoplasm.

Endosomal Uptake and Escape

In order to achieve transfection efficiency similar to that of PEI25K but with a lower molecular weight, less cytotoxic PEI carrier, endosomal escape becomes the rate limiting barrier that must be overcome efficiently (6). We focused our kinetic study on the endosomal uptake and release steps. The following temporal profiles of PEI25K, PEI1.8K, and WSLP show significantly different uptake kinetics. All three complexes readily bind to the plasma membrane. PEI25K (Fig. 2) complex undergoes rapid endosomal uptake followed by rapid release. This leads to little accumulation of the complex

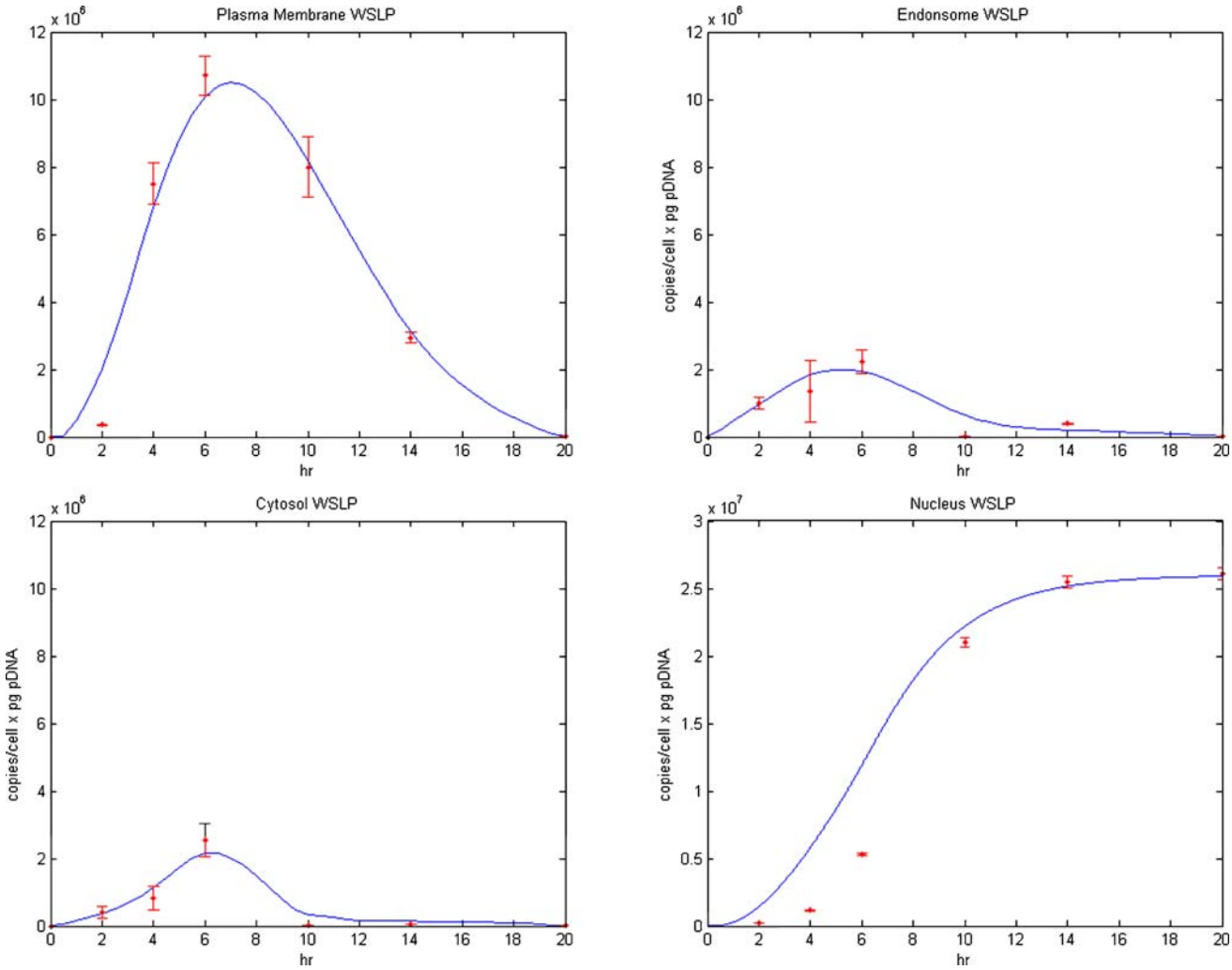

Fig. 4. Experimental result and parameter fitting curve of plasmid DNA equivalent time-lapse profile in each cellular compartment (plasma membrane, endosome, cytosol, and the nucleus). B16-F0 cells were transfected with 10 μg pCMVIL-12 complexed with WSLP followed by subcellular fractionation and isolation of the plasmid DNA. Plasmid DNA equivalent are measured using realtime-PCR. Data are reported as mean ± SD of three experiments.

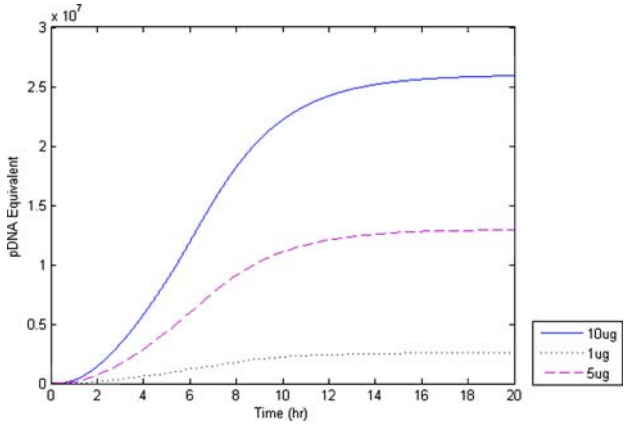

Fig. 5. Predicted nuclear accumulation with initial exposure of 1 μg, 5 μg, and 10 μg pDNA complexed with WSLP (N/P = 15/1) per 10^7 cells. The profiles increase proportionally within the exposure range.

inside the endosomes. PEI1.8K (Fig. 3) has a slower endosomal uptake and even slower endosomal release, resulting in little cytosolic accumulation of the complex for nuclear entry.

WSLP (Fig. 4) has an uptake profile similar to PEI25K. It shows significant and rapid accumulation in both endosomes and the cytosol. In comparison to that of PEI25K, the endosomal escape of WSLP is not as fast. In comparison to that of PEI1.8K, the endosomal degradation of WSLP may also be slower due to its chemical structure. It's possible that the cholesterol moieties provide a steric effect against acid and enzymatic degradation in the endosomes. Additional studies may be carried out to examine this potential effect.

Nuclear Uptake

Zetterberg and Larsson previously proposed that before a G1 phase restriction point, cells under serum starvation experience retarded division and enter G0 (10) phase. Because the sizes of our pDNA/polymer complexes (PEI25K NP5:1 220 nm, PEI1.8K NP15:1 50 nm, WSLP NP15:1 50 nm) are bigger than the typical nuclear pore (25–50 nm), it is likely that the nuclear uptake process is dependent on cell division for these high molecular weight polymer complexes. The initial transfection period (0–4 h) occurred in serum starvation condition. After the fourth hour, cell medium was replenished with 10% FBS. The rapid accumulation of the plasmid DNA inside the nucleus transfected by PEI25K occurs 2 h after the medium is replaced. Wilke *et al*. showed similar mitosis dependency with peptide based polyplexes (11). For the small molecular weight polymers however, we observe a steady accumulation of the pDNA in the nucleus fractions over the complete experimental time course.

Because none of these polymer constructs contain a nuclear localization signal, this diffusion and mitosis-dependent nuclear uptake should be a function of total availability of pDNA and not chemical difference in our polymer carriers in our study. Our analysis reveals that the difference in transfection efficiency of the three different polymers is attributed to upstream steps before nucleus entry. Because the major barrier for PEI1.8K appears to be endosomal escape, the nucleus accumulation of the pDNA after the 10 h time point is significantly less than that of PEI25K. However, after the chemical modification of PEI1.8K to WSLP, a greater nuclear accumulation of the pDNA occurs suggesting the ability to overcome this barrier as a result of the polymer modification.

Additionally, we evaluated the effect of exposure on the nuclear uptake of the pDNA. Figure 5 hows the predicted plasmid DNA accumulation inside the nucleus with WSLP as a carrier. The increase in the nuclear uptake follows the increase in initial exposure proportionally. This is encouraging because it provides a way to approximate required dosage in these delivery systems to reach intended therapeutic window.

Model Analysis

We constructed a reaction model to characterize the steps of intracellular gene delivery. For parameter estimation and model optimization, we use the Nelder-Mead simplex method. The Nelder-Mead simplex method (12), first published in 1965, for unconstrained optimization has been used extensively to solve parameter estimation problems for almost 40 years. It is a direct search method that attempts to minimize a scalar non-linear function of real variables (13), without derivation information for the problem to be solved. A simultaneous fit is performed to minimize correlative interference of parameters. Each potential rate limiting step is mathematically quantified by a rate constant parameter whose values determined by our model are listed in Table I. These rate constants are likely to be carrier and cell line dependent.

The mathematical model result shows that the rate limiting barriers are different for the three polymers. The biggest rate limiting barriers for PEI25K are nuclear entry and membrane binding. The small MW polymers have an enhanced nuclear entry rate constant. The major rate limiting step for PEI1.8K complex is the endosomal escape. PEI25K has the greatest endosomal escape capability. WSLP has dramatically improved endosomal escape capability compared to that of PEI1.8K. The rate limiting barrier for this construct is endosomal uptake.

Comparing the modeling results of the three polymers, the membrane binding constants K_{MP} for the three polymers vary by three orders of magnitude. WSLP appears to have much better binding kinetics in comparison to the unmodi-

Table I. Rate Parameter Values from Model Predictions by PEI25K, PEI1.8K, and WSLP Including Membrane Binding (MP), Endosomal Uptake (PE), Endosomal Escape (EC), Nucleus Uptake (CN) and Degradation in the Plasma Membrane (dP), Endosome/Lysosome (dE), and Inside the Cytoplasm (dC)

Rate h^{-1}	PEI25K	PEI1.8K	WSLP
K_{MP}	6.527e-04	1.000e-03	3.484e-01
K_{PE}	5.018e-01	1.674e-01	2.275e-01
K_{dP}	7.200e-03	8.300e-03	7.700e-03
K_{EC}	9.343e + 01	1.000e-04	5.840e-01
K_{dE}	5.931e-01	7.4861e00	1.556e-04
K_{CN}	8.750e-02	3.540e00	2.135e00
K_{dC}	4.609e00	4.377e00	1.148e00

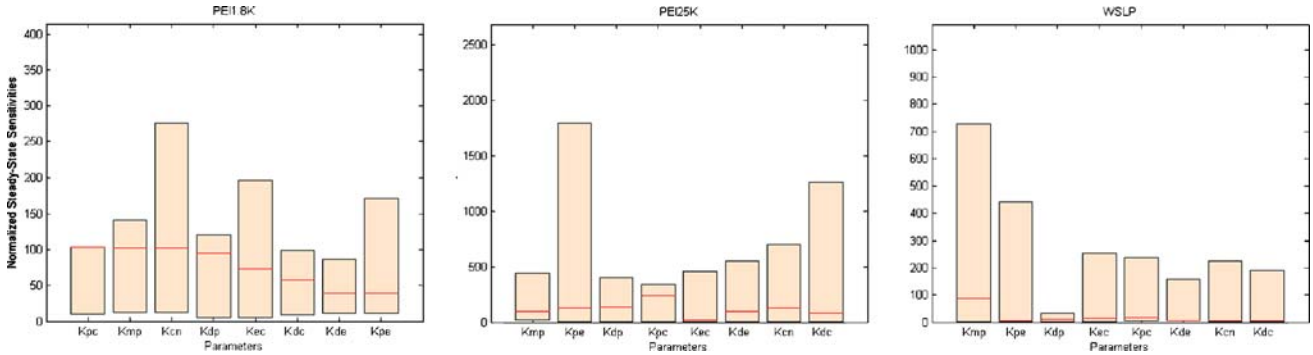

Fig. 6. Relative steady-state sensitivies (normalized by the steady-state values of the system) of PEI25K, PEI1.8K, and WSLP polymer constructs with respect to each of the model parameters. The parameter with the highest sensitivity value represents rate limiting step.

fied PEI polymers. This may be related to different levels of electrostatic interaction between the polymer complex and charged glycolipids on the cell surface. The ζ potentials for PEI25K, PEI1.8K and WSLP are 4 mV, 38 mV, and 49 mV respectively. The endosomal uptake rates are similar for all three polymers. PEI25K has a rapid endosomal release, resulting in little residual endosomal accumulation of the pDNA/polymer complex. The most dramatic increase due to the chemical modification is observed with the endosomal release rate constant, K_{EC}. PEI1.8K has a K_{EC} of 1.000e-04 while K_{EC} of WSLP is 5.840e-01, a nearly 6,000 fold increase. This is consistent with the original design intent of the WSLP to incorporate the membrane disrupting cholesteryl group. The nuclear uptake rate constant K_{CN} differs between the high molecular weight and low molecular weight polymers. As previously discussed, nuclear uptake of PEI25K complexes are largely mitosis dependent whereas the smaller molecular weight complexes may be able to enter the nucleus through a diffusive process. The plateau in the nuclear fraction with WSLP is also consistent with the rapid rate of the preceding processes compared to the other PEI complexes.

For PEI25K and WSLP transfected pDNA, the most significant degradation occurs in the cytosol, with a half life of about 2 h. Cytoplamic half life of circular pDNA due to cytosolic nuclease activity is about 1 h (14). Thus the polymers are providing some protection to the pDNA inside the cytoplasm. pDNA transfected by PEI1.8K has a cytoplasmic half life of 1 h. However, a significant portion of PEI1.8K is degraded inside the endosomes, likely due to its inability to escape. WSLP has a much smaller degradation rate in the endosomes. pDNA transfected by WSLP has an endosomal half life of about 5 h. This may be a result of the chemical modification, in addition to its ability to escape the endosomes quickly.

Sensitivity Analysis

We also performed local sensitivity analysis for our model parameter of the three polymers. Each parameter was disturbed by 10% to determine the perturbation impact on steady state nuclear concentration of the plasmid DNA. Sensitivity value quantifies the relationship between changes in a parameter and the steady state of the system. The kinetic parameter with the greatest sensitivity, indicating the steady state is affected the most by this step in the reaction, represents the rate limiting step. We normalize the magnitude of the parameters by the steady-state values to obtain relative sensitivity analysis (Fig. 6). The steady-state for each of the three polymers constructs is sensitive to a different set of parameters.

Figure 6 shows that PEI25K is most sensitive to internalization K_{PE} and nucleus uptake K_{CN} indicating these are the two possible rate-limiting barriers as targets for optimization. Better nuclear uptake can be potentially achieved by incorporation of a nuclear localization signal into the carrier. This was also suggested previously by Varga *et al.* (6). Better internalization can be achieved by

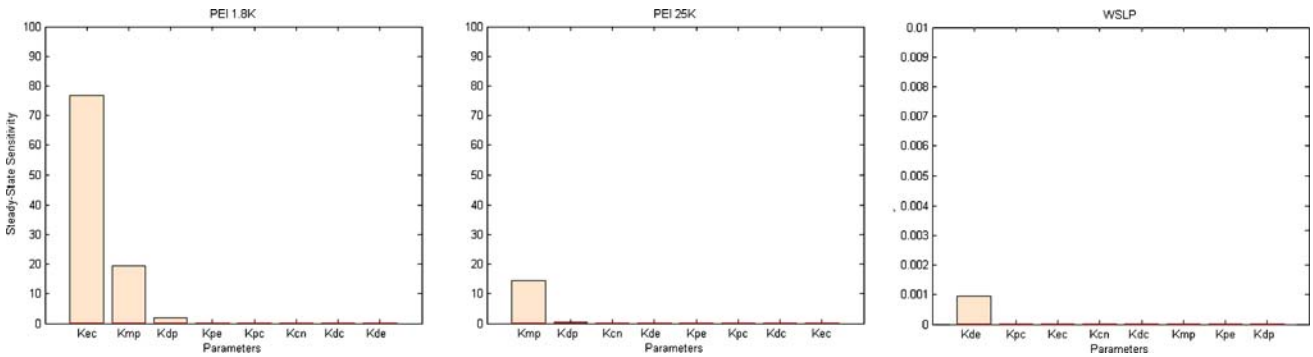

Fig. 7. Absolute sensitivity of steady state nuclear uptake with PEI25K, PEI1.8K, and WSLP constructs with respect to each model parameter. The result indicate the model parameters upon which the simulation results are most dependent.

incorporating a receptor binding ligand to facilitate receptor mediated endocytosis.

For PEI1.8K, the rate limiting steps appear to be endosomal release and nuclear uptake. Similarly to PEI25K, a nuclear localization signal can be incorporated into the polymer construct to improve nuclear uptake. Enhanced endosomal release was the objective in mind when WSLP was first designed. The chemically modified polymer now shows sensitivity to membrane binding and endosomal uptake of the bound complexes as the new rate limiting step instead of endosomal escape. To facilitate better membrane binding and endosomal uptake, receptor binding ligands can be incorporated into the WSLP polymer. This also is exemplified by our absolute sensitivity analysis as shown in Fig. 7. The steady-state of PEI1.8K complexes is most sensitive to the rate of endosomal escape K_{EC}. This sensitivity is diminished in the WSLP construct. In addition, sensitivity values of WSLP are orders of magnitude smaller than that of the other polymers. This helps to explain better delivery kinetics of WSLP than the other two polymers.

DISCUSSION

High molecular weight PEI such as PEI25K has endosomal buffering capacity producing proton accumulation followed by passive chloride influx into endosomes (15). This results in osmotic swelling and subsequent endosome disruption allowing pDNA to escape the endosomes. However, high molecular weight PEI is highly toxic to cells even at low N/P ratios. Low molecular weight PEI1.8K exhibits much lower transfection efficiency than PEI25K. The complex binds to the membrane but little endosomal or cytoplasmic accumulation occurs. It is possible that the small particle size does not destabilize the membrane sufficiently for endosomal formation. Also, PEI1.8K lacks endosomal buffering capacity due to low amine content, preventing it from quickly escaping into the cytosol. The addition of the cholesterol group to PEI1.8K to create WSLP exhibited much higher transfection efficiency similar to that of PEI25K despite having less charge density. Transfection and kinetic model data appear to support what was previously suggested that the WSLP polymer modification results in endosomal destabilization and therefore overall rate of cellular uptake (3).

Kinetic modeling showed that for high molecular weight PEI25K, nuclear entry is the rate limiting step in gene delivery. Design optimization of this carrier focused on incorporating nuclear localization signals would enhance nuclear uptake. Endosomal uptake is another rate limiting step. Incorporating targeting ligands in the polymer may enhance receptor mediated endocytosis in addition to the clathrin dependent endocytosis mechanism upon which it normally relies. For smaller molecular weight polymers such as PEI1.8K, endosomal escape is the rate limiting barrier. Endosomal degradation, a direct result of long residual time inside the endosomes, also impedes successful plasmid DNA delivery. WSLP was designed specifically to enhance the endosomal escape capability of the polymer. Sensitivity analysis of the system model shows that endosomal release is no longer the rate limiting barrier. The modification increased the rate of endosomal escape by almost 6,000 fold. The sensitivity analysis also indicates that membrane binding and endosomal uptake of the bound complexes are the rate limiting steps. Membrane binding is somewhat exposure dependent. This gives confidence that WSLP is a more likely candidate for dosage optimization rather than additional chemical structural design optimization.

There are several limitations to our model. First, we are not distinguishing different stages of endosomes. The recycling of endosomes may be embedded in both Kmp and Kde. This can be one of the limitations of the model. Additional parameter representing this mechanism can be incorporated in a study in which stages of endosomes are differentiated. In the current study, dE/dt is a global indicator of rate overcoming this barrier. Second, the model in the current study does not elucidate some of the specific intracellular mechanisms. For example, with regards to cytoplasmic transport, studies have suggested that the dense molecular network in the cytoplasm may impede the migration of complexes into the nucleus (16–18). Diffusion of large particles in the cytoplasm to the nucleic acid rich region is very limited (19–21). Several studies have suggested active transport of positively charged polyplexes by microtubules and microfilaments (22–24). Because all three PEI complexes in this study have excessive cationic charge, we expect a combination of the energy dependent mechanism and diffusion present in cytoplasmic transport. The rate parameter therefore becomes a global indicator for this step by encompassing both mechanisms.

Our quantitative study of PEI formulations for gene delivery allowed us to explore the effect of polymer physiochemical properties on its cellular delivery kinetics. The optimization in both design and dosage require understanding of the underlying mechanisms of the gene delivery process. By identifying rate limiting barriers of each formulation, optimization effort can be more focused, leading to more effective research results. We can scale up our model into a tissue based *in vivo* model where cellular exposure can be extrapolated from experimental design. Using this model, we can design *in vivo* dosage to achieve optimal cellular exposure and transfection.

ACKNOWLEDGEMENTS

We acknowledge financial supports from the National Institute of Health (CA-107070). We are grateful to Dr. Jerry Kaplan of Pathology and Dr. Maureen Condic of Neurobiology and Anatomy for their help.

REFERENCES

1. D. Fischer, *et al. In vitro* cytotoxicity testing of polycations: influence of polymer structure on cell viability and hemolysis. *Biomaterials* **24**:1121–1131 (2003).
2. H. Petersen, *et al.* Polyethylenimine-graft-poly(ethylene glycol) copolymers: influence of copolymer block structure on DNA complexation and biological activities as gene delivery system. *Bioconjug. Chem.* **13**:845–854 (2002).
3. S. Han, R. I. Mahato, and S. W. Kim. Water-soluble lipopolymer for gene delivery. *Bioconjug. Chem.* **12**:337–345 (2001).
4. T. S. Ledley and F. D. Ledley. Multicompartment, numerical

model of cellular events in the pharmacokinetics of gene therapies. *Hum. Gene Ther.* **5**:679–691 (1994).
5. G. A. Banks, R. J. Roselli, R. Chen, and T. D. Giorgio. A model for the analysis of nonviral gene therapy. *Gene Ther.* **10**: 1766–1775 (2003).
6. C. M. Varga, *et al.* Quantitative comparison of polyethylenimine formulations and adenoviral vectors in terms of intracellular gene delivery processes. *Gene Ther.* **12**:1023–1032 (2005).
7. C. M. Varga, T. J. Wickham, and D. A. Lauffenburger. Receptor-mediated targeting of gene delivery vectors: insights from molecular mechanisms for improved vehicle design. *Biotechnol. Bioeng.* **70**:593–605 (2000).
8. R. I. Mahato, *et al.* Intratumoral delivery of p2CMVmIL-12 using water-soluble lipopolymers. *Mol. Ther.* **4**:130–138 (2001).
9. D. Y. Furgeson, W. S. Chan, J. W. Yockman, and S. W. Kim. Modified linear polyethylenimine-cholesterol conjugates for DNA complexation. *Bioconjug. Chem.* **14**:840–847 (2003).
10. O. Larsson and A. Zetterberg. Existence of a commitment program for mitosis in early G1 in tumour cells. *Cell Prolif.* **28**:33–43 (1995).
11. M. Wilke, *et al.* Efficacy of a peptide-based gene delivery system depends on mitotic activity. *Gene Ther.* **3**:1133–1142 (1996).
12. J. A. Nelder and R. Mead. A simplex method for function minimization. *Comput. J.* **7**:308–313 (1965).
13. V. Torczon. On the convergence of pattern search algorithms. *SIAM J. Optim.* **7**:1–25 (1997).
14. D. Lechardeur, *et al.* Metabolic instability of plasmid DNA in the cytosol: a potential barrier to gene transfer. *Gene Ther.* **6**:482–497 (1999).
15. O. Boussif, *et al.* A versatile vector for gene and oligonucleotide transfer into cells in culture and *in vivo*: polyethylenimine. *Proc. Natl. Acad. Sci. USA.* **92**:7297–7301 (1995).
16. M. R. Capecchi. High efficiency transformation by direct microinjection of DNA into cultured mammalian cells. *Cell* **22**:479–488 (1980).
17. G. L. Lukacs, et al. Size-dependent DNA mobility in cytoplasm and nucleus. *J. Biol. Chem.* **275**:1625–1629 (2000).
18. K. Luby-Phelps. Cytoarchitecture and physical properties of cytoplasm: volume, viscosity, diffusion, intracellular surface area. *Int. Rev. Cytol.* **192**:189–221 (2000).
19. K. Luby-Phelps, P. E. Castle, D. L. Taylor, and F. Lanni. Hindered diffusion of inert tracer particles in the cytoplasm of mouse 3T3 cells. *Proc. Natl. Acad. Sci. USA* **84**:4910–4913 (1987).
20. O. Seksek, J. Biwersi, and A. S. Verkman. Translational diffusion of macromolecule-sized solutes in cytoplasm and nucleus. *J. Cell Biol.* **138**:131–142 (1997).
21. D. Lechardeur, A. S. Verkman, and G. L. Lukacs. Intracellular routing of plasmid DNA during non-viral gene transfer. *Adv. Drug Deliv. Rev.* **57**:755–767 (2005).
22. S. C. De Smedt, J. Demeester, and W. E. Hennink. Cationic polymer based gene delivery systems. *Pharm. Res.* **17**:113–126 (2000).
23. H. Pollard, et al. Polyethylenimine but not cationic lipids promotes transgene delivery to the nucleus in mammalian cells. *J. Biol. Chem.* **273**:7507–7511 (1998).
24. C. M. Wiethoff and C. R. Middaugh. Barriers to nonviral gene delivery. *J. Pharm. Sci.* **92**:203–217 (2003).